

## Phase transitions of 1,2-cyclohexanediol isomers studied by polarised light microscopy and differential thermal analysis

Maria Luísa Planas Leitão<sup>a,\*</sup>, Ricardo A.E. Castro<sup>b</sup>, Felisbela S. Costa<sup>b</sup>, J.S. Redinha<sup>a</sup>

<sup>a</sup>Departamento de Química, Universidade de Coimbra, 3004-535 Coimbra, Portugal

<sup>b</sup>Faculdade de Farmácia, Universidade de Coimbra, 3000-295 Coimbra, Portugal

Received 25 August 2000; received in revised form 7 February 2001; accepted 29 May 2001

### Abstract

Polarised light microscopy and DTA have been used to study the phase transitions observed in *cis* and *trans*-1,2-cyclohexanediol during heating/cooling cycles performed between ambient and melting temperatures to prove that the presence of impurities even in trace amounts can affect the thermal properties of the substances. Good quality commercial material before and after further purification were used in this study. © 2001 Elsevier Science B.V. All rights reserved.

**Keywords:** 1,2-Cyclohexanediol; Phase transitions; Impurities; Thermomicroscopy; DTA

### 1. Introduction

1,2-Cyclohexanediol can exist in *cis* and *trans* configuration. In the former one hydroxyl group is equatorial and the other axial relatively to the cyclohexane ring, whereas in the latter both hydroxyls are equatorially oriented. The *trans* isomer has two enantiomeric forms whose absolute configurations are (1*R*,2*R*) and (1*S*,2*S*). In a previous publication these isomers were the subject of a study using DSC and solution calorimetry [1]. In the present paper thermo-optical data for these substances are reported with a view to further interpret the thermodynamic properties in structural terms. Indeed, microscopical observation with polarised light gives a straightforward characterisation of the phases allowing their behaviour with temperature to be followed. Thus, detailed features concerning rate of phase transitions, composition diagrams, degree of stability of the metastable forms,

polymorphism, purity and so forth can be followed throughout by this method [2–4]. As pointed out in several original research papers and reviews [5–7], advances in computer use and technology have been instrumental for thermomicroscopy remaining unique in the characterization of phase transitions and for its ever increasing applications. As the hot stage used has a differential thermal analysis sensor, DTA curves were recorded simultaneously with microscopical observation. The association of the two methods allows a deeper insight into the structure of phases and an evaluation of the energy involved in their transformations.

Besides the structural aims referred above, this work also intends to stress the effect of impurities even when present in trace amounts.

### 2. Material and methods

*Cis*-1,2-cyclohexanediol, labelled as  $\geq 99\%$  pure, was purchased from Aldrich, and the *trans* enantiomers

\* Corresponding author. Fax: +351-239-827703.  
E-mail address: mlleitao@ci.uc.pt (M.L.P. Leitão).

from Fluka with purity specification >99%. The weight of the residue left after subliming the compounds used do not exceed the specified limits given by the suppliers for purity. Studies were carried out using two sort of samples, the substance used without further purification but dried at 50°C under vacuum, and after sublimation by a cold finger technique.

Thermomicroscopy was performed with a polarised light microscope fitted with a hot stage. The thermal assembly used a Mettler Toledo, FP900 equipment, consisting of a FP90 central processor unit and FP84 specimen holder. A five gold–nickel thermocouple arrangement provides the evaluation of the temperature difference between the cell containing the sample and that of the reference. Thus, with this hot stage microscope in addition to image recording, DTA following heating and cooling processes were also obtained.

The instrument used for optical observation consisted of a Leica DMRB polarising microscope connected to a Sony image processing equipment composed of CCD video camera, video recorder, video monitor and colour video printer. The sample was observed by the microscope, projected on the screen or recorded in a videocassette for later detailed examination. Sequences of up to 16 images can be printed in a photoshop format.

A digital video editing equipment on computer, studio DC10 Plus from Pinnacle Systems was used for videocapturing and creating digital movies. The image analysis was a significant advance gained from the experiments, as single frame capturing collection could be registered at critical moments. Images viewed at time intervals as low as 0.04 s can be obtained. The position of a crystal front arisen from a phase modification can be localised at any moment through Micrografx Designer 4.0a software so that the velocity of the transformation (VT) could be determined.

Temperature readings of the central processor unit were checked by determining the melting point of benzophenone (calibration substance, Mettler–Toledo,  $t_{\text{fus}} = 48.1 \pm 0.2^\circ\text{C}$ ) and benzoic acid (certified reference material, LGC 2606,  $t_{\text{fus}} = 122.35 \pm 0.03^\circ\text{C}$ ). The values obtained for these standards were  $48.1 \pm 0.2^\circ\text{C}$  and  $122.3 \pm 0.2^\circ\text{C}$ , respectively. Uncertainty corresponds to 95% confidence interval and based on five determinations. Benzoic acid was also used

for quality assurance of DTA method. The heating rate could be controlled between 0 and  $20^\circ\text{C min}^{-1}$ . Cooling is carried out by cold airflow. The heating rate was usually  $10^\circ\text{C min}^{-1}$  and the cooling rate was  $4^\circ\text{C min}^{-1}$ .

A small amount of the substance to be studied was placed in a glass crucible used as cell, which was covered with a glass lid. Care was taken in order to have in the cell solid particles apart from each other. This procedure allows to follow what happens to each solid particle during heating and cooling, in successive thermal cycles. An empty glass crucible identical to that of the sample was used as the reference cell. Any sample was submitted to five heating/cooling cycles between room temperature and the melting point and for each substance five samples were taken.

Thermal cycles were usually followed by  $50\times$  magnification in order to have a few particles under microscopical observation. A  $200\times$  magnification was used only for detailed observation. The size of the particles varied within a range from hundredths to tenths of a millimeter.

### 3. Results and discussion

#### 3.1. *Cis*-1,2-cyclohexanediol

The images of the phases found for *cis* isomer during heating and cooling runs performed between 20 and  $110^\circ\text{C}$  are shown in Fig. 1a.

When the crystalline form is heated from 20 to  $91^\circ\text{C}$  only one birefringent phase is observed. As the temperature reaches this value an isotropic solid phase is formed which in turn melts at about  $100^\circ\text{C}$ .

Three well-defined phase transitions were observed when the melt is cooled. Firstly, the liquid gives rise to the isotropic solid phase found on heating; secondly, this phase gives rise to an anisotropic solid with a coloured striated texture which is afterwards converted into the stable crystalline form. Numbering the phases according to the order of appearance from the melt, one can summarise the thermal cycle on that by cooling the molten *cis*-1,2-cyclohexanediol gives crystalline forms I, II and III and on heating only crystal III and I are observed.

The values of the temperature, at which the phase transition just begins,  $t_i$ , are presented in Table 1. DTA

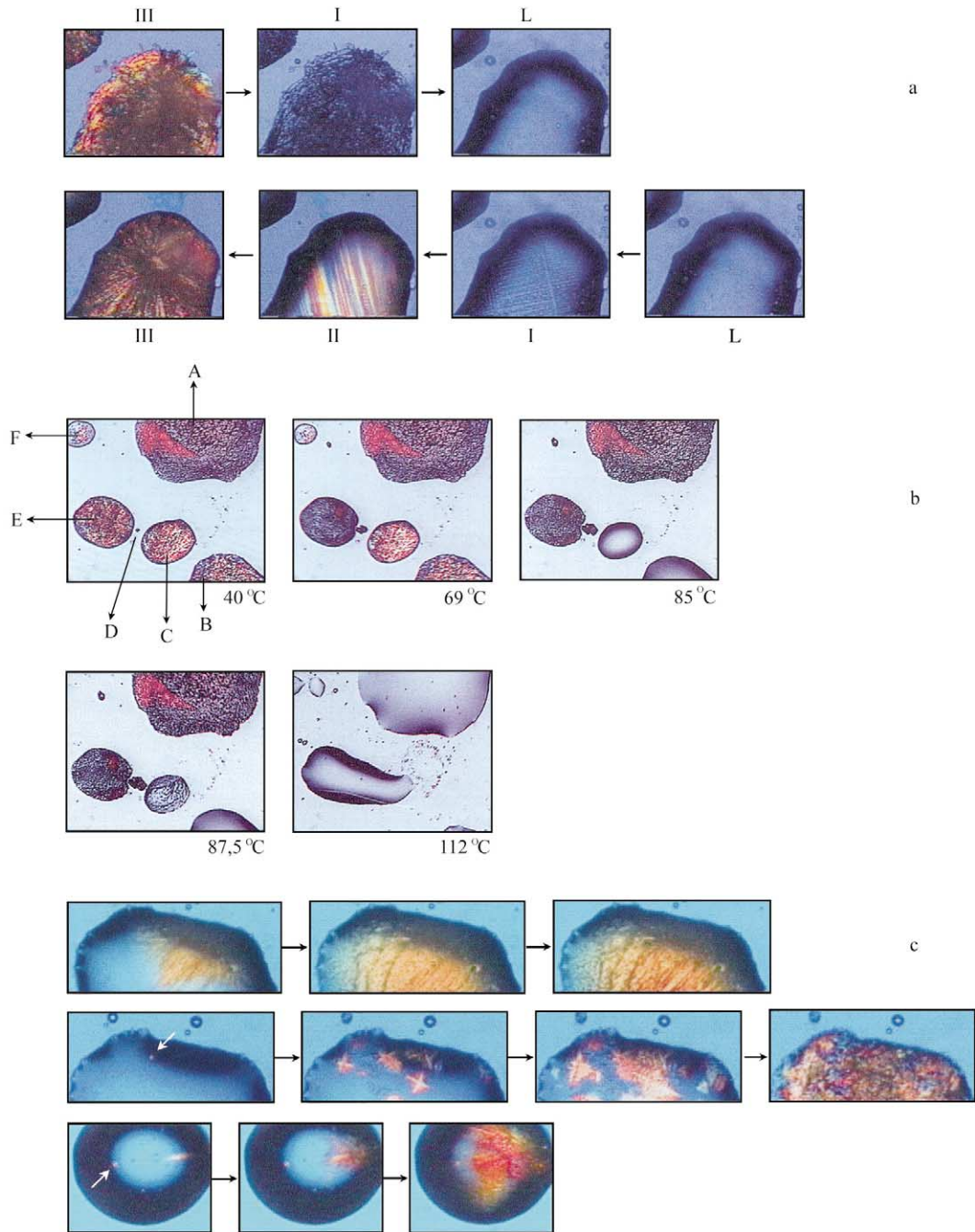


Fig. 1. Phase transition observed for 1,2-cyclohexanediol isomers. (a) *Cis*-1,2-cyclohexanediol during heating and cooling runs; (b) Types of transition occurring during the heating run of *trans*-(1*R*,2*R*)-cyclohexanediol; (c) Crystallization of *trans*-(1*R*,2*R*)-cyclohexanediol from melt leading to high- and low-melting phases and to a mixture.

Table 1  
Phase transition temperature for *cis*-1,2-cyclohexanediol

Process	Phase transition	$t_i$ (°C)
Heating	III → I	91.0 ± 0.4
	I → L	99.3 ± 0.3
Cooling	L → I	96.7 ± 0.5
	I → II	74.2 ± 0.1
	II → III	48–43

curves of heating and cooling runs are presented in Fig. 2. The features of these curves are in close agreement with the data given by thermomicroscopy.

Fig. 3 provides a thermochemical phase diagram description of *cis*-1,2-cyclohexanediol. A discussion of this diagram in structural terms will be now undertaken.

X-ray diffraction study proves that crystal III belongs to the orthorhombic crystallographic system and that hydrogen bonding plays an important role in the structural organisation [8]. This can be described as layers of dimers held together in a three-dimensional network by interdimeric hydrogen bonds. Under polarised light this phase gives, in fact, a microscopical image of a birefringent crystal.

On increasing the temperature, crystal III is transformed into crystal I. The transition process nucleated

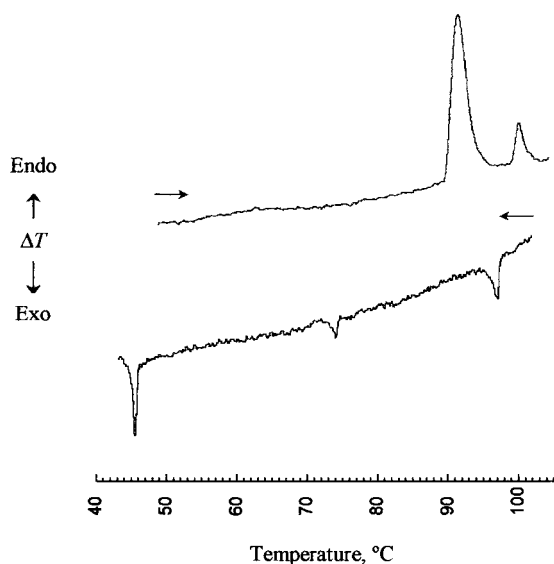


Fig. 2. Heating and cooling DTA curves for *cis*-1,2-cyclohexanediol.

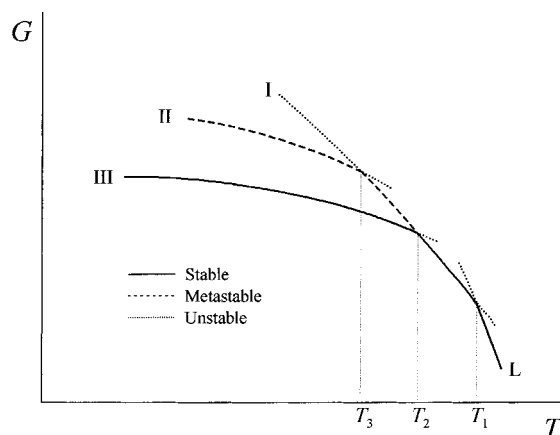


Fig. 3. Gibbs energy as function of temperature for *cis*-1,2-cyclohexanediol.

on the crystal surface and grows towards the centre with a VT value of  $7 \times 10^{-3} \text{ cm s}^{-1}$ . The microscopical observation shows a loss of colour of the mother phase without any apparent modification of its texture. The fusion of crystal I is the transformation of the solid into the liquid.

Taking the thermomicroscopic data and the relative peak areas of DTA curves together, one concludes that crystal III/crystal I is an order/disorder transition involving high values of enthalpy and entropy. By increasing the temperature some hydrogen bonds become weak and the molecular energy overcomes the intermolecular barrier allowing librational motions. The new phase, often called plastic crystal, solid rotator phase or orientationally disordered phase, has a structure resembling that of the liquid as far as no long range molecular order exists but like a solid no molecular translational motion occurs [9–12]. For some authors it is considered as a meso-phase intermediate between an isotropic liquid and a true crystalline solid [13,15,16]. The optical isotropy shows that this is not a smectic or nematic liquid crystal. It is still the structural likeness of the crystal I and the liquid state that accounts for the small value of enthalpy and entropy of the melting process.

The sequence of states observed on cooling the melt is interpreted as follows. The supercooled liquid gives rise to crystal I. Solidification is a fast process growing from the initial nucleus to dendrites with a VT value of  $2 \times 10^{-1} \text{ cm s}^{-1}$ . The difference of 2.6°C between the melting point of crystal I and the freezing temperature

of the melt is a low degree of supercooling which indicates again that crystal I is a frozen disordered liquid structure. Under high supercooling conditions crystal I is transformed into crystal II with a VT value of  $8.1 \times 10^{-2} \text{ cm s}^{-1}$ . This crystalline modification presents a longitudinal edge striation texture similar to that shown by some inorganic systems and ascribed to perturbation at the growth interface due to turbulent convection [14]. This new form lasts for several hours, even days when maintained at a temperature around  $70^\circ\text{C}$  but it decays into crystal III at a temperature value between  $60$  and  $40^\circ\text{C}$  and it is converted into crystal I at  $80^\circ\text{C}$ . It is to be noted that, in spite of a very small energy involved, crystal I/crystal II is a conversion of a disordered into a more ordered state. Crystal II is therefore the intermediate state of the transformation of an orientationally disordered crystal I into a stable crystal III. In a first step the molecules pass to an orientationally organised state under a relatively weak intermolecular forces and then, as temperature decreases, a second transition gives rise to the tightly packed, crystal III. This phase grows from a nucleus at a VT of  $9 \times 10^{-3} \text{ cm s}^{-1}$ .

### 3.2. *Trans*-(1*R*,2*R*)-cyclohexanediol

*Trans*-(1*R*,2*R*)-cyclohexanediol with a purity level of 99% showed on first heating no phase transition but only fusion. However, two kinds of behaviour for the particles were subsequently observed. Some of them melted at a temperature around  $80^\circ\text{C}$  whereas others melt at about  $107^\circ\text{C}$ . The two types of particles had different colours and textures under polarised light microscopy. The low or high melting temperature modification was not inherent to a particular particle since in successive heating/cooling cycles a particle would randomly present either of these behaviour patterns.

Fig. 1b illustrates the phenomena that occur when a cold molten sample was heated. Particles A and D are high-melting and the others are low-melting forms. The size of the particles ranged from 0.07 to 0.5 mm. As the temperature increased the size of D increased due to the condensation of vapour onto its surface from the low-melting form. Sublimation, as seen from a decrease in the size of the particles, was also observed. As particle D contacted E, as in the experiment at  $69^\circ\text{C}$ , a sudden transformation of this into the

high-melting form was seen. At  $80^\circ\text{C}$ , particles B, C and F melt and the resulting liquid drops can have different ends. Whilst B and F remain in the liquid state to fusion temperature, C came in contact with D at  $87.5^\circ\text{C}$ , and crystallised. Finally fusion of A, C, D and E is observed.

The observations registered during heating proved that the solid obtained from the melt is a system composed of a low- and a high-melting phase. The first is unstable and can decay into the higher-melting form from vapour/solid, solid/solid or liquid/solid transition either nucleated in the high-melting phase which was stable in this temperature. The first involved vapour from sublimation or vaporisation of the low-melting modification at temperatures from a few degrees below its melting point upwards; the vapour deposition on the surface of the stable phase particles increases the probability of contact with liquid or solid unstable phase more probable. The second type of transition, depending on the packing of the powder under testing, is also observed at temperatures not far below the melting of the unstable phase. As the liquid has a higher mobility than the solid the probability of contact with a stable phase is higher and this makes the last transition more frequent than the second.

As at room temperature both phases coexist and the unstable modification behaves as a metastable phase. For a powder sample packed in a cell maintained at  $100^\circ\text{C}$  for say 15 min, the conversion into a stable form is almost complete.

Freezing the melt provides valuable information on the nature of the phases of this enantiomer. Two kinds of crystallisation processes were observed. In some liquid droplets the crystallisation is characterised by a fast diffusion crystal front spread from a nucleus in the surface with a VT value of  $0.4 \text{ cm s}^{-1}$ . After solidification is over, small segregated portions of liquid crystallise through a nucleationless process, which takes 20–30 s to be accomplished. This mechanism gives rise to the high-melting form, called crystal I. In some other droplets the new phase formation commences on a nucleus which gives rise to tetrahedral crystallisation fronts progressing at a VT of  $1.8 \times 10^{-3} \text{ cm s}^{-1}$  along the tetrahedron corner directions. The number of nuclei is variable from one particle to the other. The crystal fronts do not overlap. Just as this stage of solidification is over, the particle

Table 2  
Phase transition temperature for *trans*-(1*R*,2*R*)-cyclohexanediol 99% pure

Process	Phase transition	$t_i$ (°C)
Heating	I → L	106.9 ± 1.0
	II → L	79.6 ± 1.0
Cooling	L → I, II	50–58

surface is covered with a thin layer of a solid phase growing at a  $0.2 \text{ cm s}^{-1}$  by a diffusing process. This sluggish process leads to the low-melting solid modification crystal II. In some cases mixed crystallisation can be observed. Solidification occurs as crystal II until crystal I formation is initiated and becomes dominant. The three nucleation-growth processes are illustrated in Fig. 1c. The temperature values for the phase transition are given in Table 2.

Fig. 4 contains typical DTA curves observed during heating and cooling. They illustrate very well the different phase transformations observed by microscopy. Curves 1 and 3 show the fusion peaks of the two phases present in the sample at different proportions; curve 4 regards a heating process in which the endothermic peak due to the fusion of the crystal II form is followed by an exothermic transformation which corresponds to crystallisation of the liquid into a high-melting solid; curve 5 shows a solid/solid transition, which gives rise to an exothermic peak prior to melting.

Freezing is accompanied throughout two or three narrow exotherms at temperatures enclosed in the interval referred to on Table 2. Although crystal II shows a tendency for crystallising before crystal I this cannot be taken to be a rule.

The metastable phase of this enantiomeric form of *trans*-cyclohexanediol has been identified for the first time and no other properties are known besides those quoted in the present work. The structure of the stable phase was studied by X-ray diffractometry and showed a trigonal crystallographic unit cell [17].

Following the procedure used for 99% pure sample, experiments with sublimed *trans*-(1*R*,2*R*)-cyclohexanediol were carried out. The values obtained for the phase transition temperatures are listed in Table 3.

The main differences observed for the sublimed samples relatively to those of 99% purity can be summarised as follows. Crystallisation of the molten

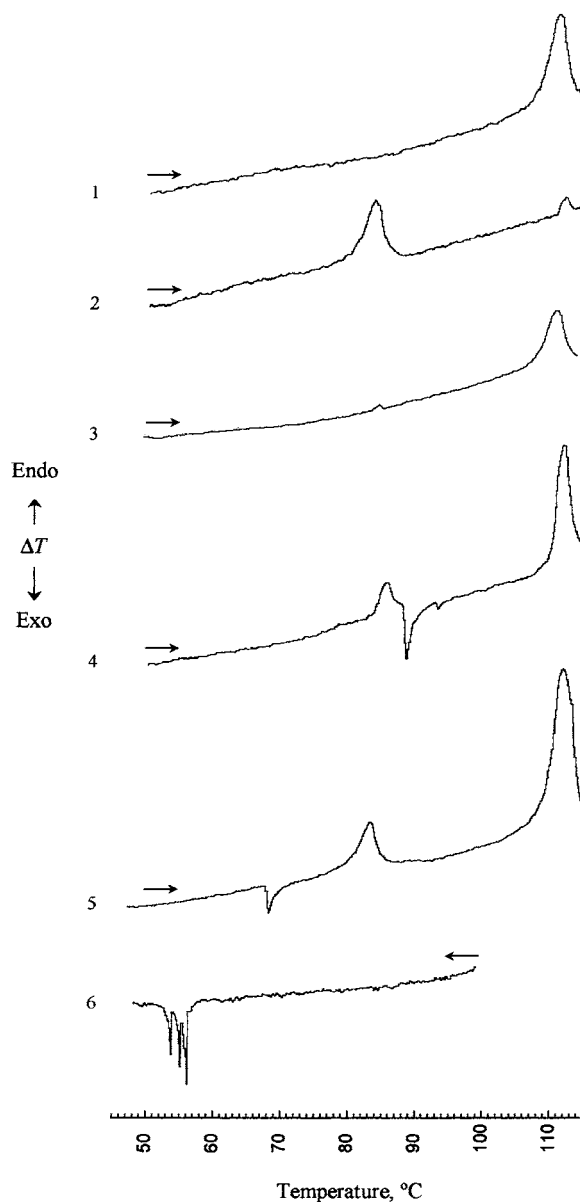


Fig. 4. Heating and cooling DTA curves for *trans*-(1*R*,2*R*)-cyclohexanediol.

state gives fundamentally crystal I on cooling; some particles with texture typical of crystal II are sometimes formed through a mechanism not apparently different from that leading to crystal I. The fusion temperature of both phases are about 3°C higher and the fusion peaks are narrower. The crystallisation on supercooling for crystal II from the melt occurs at

Table 3  
Phase transition temperature for sublimed *trans*-(1*R*,2*R*)-cyclohexanediol

Process	Phase transition	$t_i$ (°C)
Heating	I → L	110.0 ± 0.4
	II → L	83.3 ± 0.2
Cooling	L → I, II	67–69

almost 10°C lower. The DTA curves are always of type 1 or 3 as show in Fig. 4.

It is quite impossible to know whether or not the behaviour exhibited by the sublimed substance, in particular the formation of crystal II, is influenced by very low concentration of impurities. In any case, the results shown above point out the effect that impurities can have on the properties of a chemical compound. In the present case, besides the common effects as a contaminant, they enhance the metastable polymorphic form by interfering in the kinetics of the crystallisation processes.

As represented in Fig. 5, crystals I and II are part of a monotropic system and can coexist at room temperature for a certain time. By increasing the temperature these phases melt at temperatures  $T_1$  and  $T_2$ .

In equilibrium conditions the molten compound originate by freezing crystal I. However, the supercooling required for nucleation of this stable form is high enough to nucleate the higher energy phase, crystal II. Thence the solid obtained is composed of

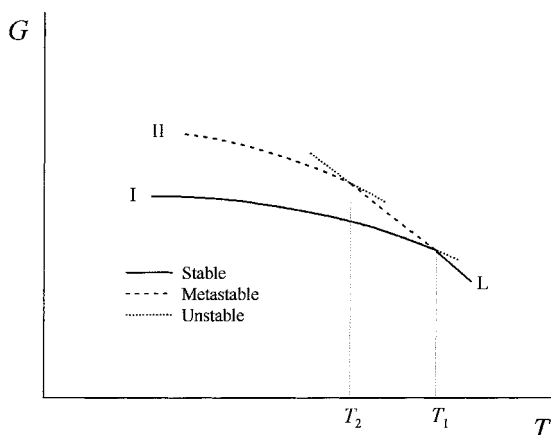


Fig. 5. Gibbs energy as function of temperature for *trans*-(1*R*,2*R*)-cyclohexanediol.

crystal I and traces of crystal II. In the presence of impurities, crystallisation is retarded and the increasing of supersaturation makes the nucleation of the two polymorphic forms competitive. Owing to this and to the difference in VT values found for the crystallisation of the two crystalline forms, mixtures of a wide range of composition by freezing are obtained. Although no satisfactory explanation has been advanced quite a few examples of retarding crystallisation due to the presence of impurities have been described. They can affect nucleation, induction time and crystal growth rate [18].

### 3.3. *Trans*-(1*S*,2*S*)-cyclohexanediol

Similar studies to these described for (1*R*,2*R*) enantiomer were performed for 99% pure and sublimed samples of *trans*-(1*S*,2*S*)-cyclohexanediol. The impurities present in the commercialised product depresses the melting point by about 4°C and give rise to broader fusion curves. The temperature values for fusion and solidification of the phases presented by sublimed *trans*-(1*S*,2*S*)-cyclohexanediol enantiomer are not significantly different from those quoted for *trans*-(1*R*,2*R*)-cyclohexanediol presented in Table 3.

In very few cases the solid obtained from the molten substance exhibit an unstable polymorph whose melting point is close to that of *trans*-(1*R*,2*R*)-cyclohexanediol. However, unlike what happens with this enantiomer the probability of forming the metastable form from 99% or sublimed *trans*-(1*S*,2*S*)-cyclohexanediol melt is about the same. This means that the nature of impurities following the two commercialised drugs is different and has different effects on the crystallisation process. Although the impurities have not been identified, the residues left on sublimation have infrared spectra different from the parent material.

## 4. Conclusion

In this work it has been shown that hot-stage microscopy is an extremely useful method of studying phase transitions. The physical characterisation of these phases viewed by polarised light microscopy together with enthalpy changes involved in the phase transformation measured by DTA gives a deeper

insight into the structure of 1,2-cyclohexanediol isomers.

The influence of trace impurities on the physical properties and on the behaviour of the systems under study requires more attention. The impurities present in 99% pure commercial *trans*-(1*R*,2*R*)-cyclohexanediol, besides depressing the melting point, increase the probability of formation of a metastable polymorphic form.

## References

- [1] T.M. Maria, F.S. Costa, M.L. Leitão, J.S. Redinha, *Thermochim. Acta* 269/270 (1995) 405.
- [2] M. Kunhert-Brandstätter, in: G. Svehla (Ed.), *Thermomicroscopy of Organic Compounds in Comprehensive Analytical Chemistry*, Elsevier, Amsterdam, 1982.
- [3] W.C. McCrone Jr., *Fusion Methods in Chemical Methods*, Interscience Publishers, New York, 1957.
- [4] M. Kunhert-Brandstätter, *Thermomicroscopy in the Analysis of Pharmaceuticals*, Pergamon Press, Oxford, 1971.
- [5] J.D. Dunitz, *Pure Appl. Chem.* 63 (1991) 177.
- [6] I.M. Vitez, A.W. Newman, M. Davidovich, C. Kiesnouski, *Thermochim. Acta* 324 (1998) 187.
- [7] P.M. Cooke, *Anal. Chem.* 72 (2000) 169R.
- [8] R. Sillampää, M. Leskelä, L. Hiltunen, *Acta Chem. Scand. B38* (1984) 249.
- [9] V.P. Kuselov, *Thermochim. Acta* 266 (1995) 129.
- [10] A. Gavezzotti, M. Simoneta, *Chem. Rev.* 82 (1982) 1.
- [11] J. Timmermans, *J. Phys. Chem. Solids* 18 (1961) 1.
- [12] A. Müller, *Proc. R. Soc. A* 138 (1932) 514.
- [13] G.W. Gray, P.A. Winsor, *Liquid Crystals and Plastic Crystals*, Ellis Horwood, Chichester, 1974 (Chapter 1).
- [14] J.R. Carruthers, *Crystal growth from the melt*, in: N.B. Hannay (Ed.), *Treatise on Solid State Chemistry*, Vol. 5, Plenum Press, New York, 1975 (Chapter 7).
- [15] W.C. Hamilton, *Mol. Cryst. Liquid Cryst.* 9 (1969) 11.
- [16] W.P. Slichter, *Mol. Cryst. Liquid Cryst.* 9 (1969) 81.
- [17] S. Hanessian, A. Gomtsyan, M. Simard, R. Roelens, *J. Am. Chem. Soc.* 116 (1994) 4495.
- [18] J.W. Mullin, *Crystallization*, Butterworth-Heinemann Ltd., Oxford, 3rd Edition, 1993 (Chapters 5 and 6).